Available online at www.sciencedirect.com
ScienceDirect
Journal of Molecular and Cellular Cardiology 41 (2006) 902–913
Journal of Molecular and Cellular Cardiology
www.elsevier.com/locate/yjmcc

Original article

Differential hypertrophic effects of cardiotrophin-1 on adult cardiomyocytes from normotensive and spontaneously hypertensive rats

Natalia López [a], Javier Díez [a,b], María Antonia Fortuño [a,*]

[a] *Division of Cardiovascular Sciences, Centre for Applied Medical Research (CIMA), Avda. Pio XII, 55. 31008, University of Navarra, Pamplona, Spain*
[b] *Department of Cardiology and Cardiovascular Surgery, University Clinic, University of Navarra, Pamplona, Spain*

Received 20 October 2005; received in revised form 9 February 2006; accepted 30 March 2006

Abstract

Cardiotrophin-1 (CT-1) produces longitudinal elongation of neonatal cardiomyocytes, but its effects in adult cardiomyocytes are not known. Recent observations indicate that CT-1 may be involved in pressure overload left ventricular hypertrophy (LVH). We investigated whether the hypertrophic effects of CT-1 are different in cardiomyocytes isolated from adult normotensive and spontaneously hypertensive rats (SHR). Hypertrophy was evaluated by planimetry and confocal microscopy, contractile proteins were quantified by Western blotting and real-time RT-PCR, and intracellular pathways were analyzed with specific chemical inhibitors. CT-1 increased c-*fos* and ANP expression ($p<0.01$) and cell area ($p<0.01$) in cardiomyocytes from both rat strains. In Wistar cells, CT-1 augmented cell length ($p<0.01$) but did not modify either the transverse diameter or cell depth. In SHR cells, CT-1 increased cell length ($p<0.05$), cell width ($p<0.01$) and cell depth, augmented the expression of myosin light chain-2v (MLC-2v) and skeletal α-actin ($p<0.01$) and enhanced MLC-2v phosphorylation ($p<0.01$). The blockade of gp130 or LIFR abolished CT-1-induced growth in the two cell types. All distinct effects observed in cardiomyocytes from SHR were mediated by STAT3. Baseline angiotensinogen expression was higher in SHR cells, and CT-1 induced a 1.7-fold and 3.2-fold increase of angiotensinogen mRNA in cardiomyocytes from Wistar rats and SHR respectively. In addition, AT1 blockade inhibited the specific effects of CT-1 in SHR cells. Finally, *ex vivo* determinations revealed that adult SHR exhibited enhanced myocardial CT-1 (mRNA and protein, $p<0.01$), increased cell width ($p<0.01$) and concentric LVH compared with pre-hypertensive SHR. These findings reveal a specific cell-broadening effect of CT-1 in cardiomyocytes from adult SHR and suggest that the hypertensive phenotype of these cells may influence the hypertrophic effects of CT-1, probably by means of an exaggerated induction of angiotensinogen expression. We suggest that CT-1 might facilitate LVH in genetic hypertension through a cross-talk with the renin–angiotensin system.

Keywords: Adult cardiomyocytes; Angiotensinogen; Cardiac hypertrophy cardiotrophin-1; Hypertension; Myofibrils; Sarcomere; STATs

1. Introduction

Left ventricular hypertrophy (LVH) is the first compensatory mechanism that the overloaded myocardium employs to maintain its normal function, and in the case of hypertensive heart disease it is an independent predictor of cardiovascular events. Pathological perpetuation of pressure overload together with non-hemodynamic factors promotes an early adaptative increase in wall thickness (concentric hypertrophy), normally followed by the reduction in myocardial distensibility and the development of dilated cardiomyopathy and heart failure [1]. At cellular level, the growth of cardiomyocytes is the main determinant of LVH, although other factors such as exaggerated collagen accumulation are also involved [2,3]. Recent experimental and clinical evidence indicates that interleukin-6-related cytokines may participate in the development of hypertensive LVH [4–6].

Cardiotrophin-1 (CT-1) is a member of interleukin-6 (IL-6) family of cytokines that exerts its cellular effects by interacting with the heterodimer constituted by the glycoprotein 130 (gp130) and the leukemia inhibitory factor receptor β (LIFR) [7]. In terminally differentiated cardiomyocytes, activation of ERK1/2 and PI3K/Akt pathways results in cell protection

* Corresponding author. Tel.: +948 19 47 00x3023; fax: +948 19 47 16.
E-mail address: fortuto@unav.es (M. Antonia Fortuño).

0022-2828/$ - see front matter © 2006 Elsevier Inc. All rights reserved.
doi:10.1016/j.yjmcc.2006.03.433

against ischemic [8] and non-ischemic death stimuli [9]. CT-1 was first cloned from embryoid bodies as a 21.5 kDa protein capable to induce hypertrophy in neonatal cardiomyocytes [10]. Subsequent studies confirmed these observations showing the involvement of signal transducers and activators of transcription (STATs) as the main signaling pathway [11]. In addition, hypertrophy induced by CT-1 in neonatal cardiomyocytes exhibits a longitudinal morphometry and a distinct molecular pattern compared to α-adrenergic stimulation [12]. The *in vitro* studies performed in neonatal cells suggesting a role for the cytokine in cardiac hypertrophy are further supported by several *in vivo* observations. First, intraperitoneal administration of recombinant CT-1 to normotensive mice increases left ventricle weight in a dose-dependent manner, although the geometric pattern of hypertrophy has not been determined [13]. Moreover, left ventricular CT-1 expression is increased in different experimental models of hypertensive LVH [5,14]. In addition, an association between LVH and high plasma levels of CT-1 has recently been observed in essential hypertensive patients [6]. Furthermore, regression of LVH and diminution of plasma levels of CT-1 are associated in treated hypertensive patients [15]. However, the hypertrophic effects of CT-1 in adult cardiomyocytes have not been investigated.

The aim of this study was to characterize the hypertrophic effects of CT-1 in adult cardiomyocytes and to investigate whether CT-1-induced hypertrophy is influenced by the hypertensive phenotype of cells. Thus, hypertrophic effects of the cytokine were analyzed in cardiomyocytes isolated from adult normotensive (Wistar) and spontaneously hypertensive rats (SHR). We also investigated the myocardial expression of CT-1 in adult SHR before and after the development of LVH.

2. Methods

2.1. Animals

The investigation was performed in accordance with the *Guide for Care and Use of Laboratory Animals* published by the US National Institutes of Health (NIH Publication no. 82-23, revised in 1996). Animals were provided by Harlam UK Limited (Bicester, England). All rats were housed in individual cages and were fed a standard rat chow and tap water *ad libitum*. They were maintained in a quiet room at constant temperature (20 to 22 °C) and humidity (50 to 60%). For the study with isolated cardiomyocytes, Wistar rats and SHR weighting 200–250 g were sacrificed by decapitation under anesthesia i.p. with Ketamine 75 mg/kg (Imalgene 1000, Merial) and Xilacine 5 mg/kg (Rompun, Bayer), and the hearts were rapidly excised for cardiomyocytes isolation. For *ex vivo* determinations, 6-week-old SHR (Control group, $N=20$) and 30-week-old SHR ($N=20$) were employed. Systolic blood pressure was measured by the standard tail-cuff method using a LE 5007 Pressure Computer (Letica Scientific Instruments). Animals were sacrificed by the protocol described above. Hearts were extracted, weighted and rapidly frozen in liquid nitrogen for molecular studies or fixed by immersion in 4% buffered formalin for 24 h and embedded in paraffin for morphometric determinations. Hence, systolic cardiac dimensions were computed by Image Analysis as described below.

2.2. Adult cardiomyocyte isolation and culture

Primary cultures of adult cardiomyocytes were obtained as recently described [9]. Briefly, the hearts were perfused on a Langerdorff system at 37 °C with a calcium-free buffer (115 mmol/L NaCl, 2.6 mmol/L KCl, 1.2 mmol/L $MgSO_4$, 1.2 mmol/L KH_2PO_4, 6 mmol/L $NaHCO_3$, 11 mmol/L glucose (D+), pH 7.3) and Collagenase A (Boehringer–Mannheim) at 0.2% (w/v). Left ventricles were minced into small pieces in oxygenated perfusion buffer with BSA 1.3% and trypsin 0.025% and then centrifuged at $50\times g$ for 5 min. Following the enrichment step with 4% BSA, cells recovered from the pellet consisted of 90% rod-shaped viable cardiomyocytes. The average number of cardiomyocytes obtained was 2.5×10^6. Cells were plated in laminin-pre-coated (0.5 μg/cm^2) culture plates at a density of 10^4 cells/cm^2 in serum-free medium 199 with Hanks' salts supplemented with 26 mmol/L $NaHCO_3$, 10^{-4} mmol/L insulin, 5 mmol/L creatinine, 2 mmol/L L-carnitine, 0.2% BSA, 10^{-5} mmol/L Ara-C, 5 mmol/L taurine, 100 IU/mL penicillin, 0.1 mg/mL streptomycin, 10 mmol/L *N*-(2-hydroxyetil) piperazine-*N*′2-etanolsulfonic acid (HEPES), pH 7.4. After 4 h of pre-incubation, attached cells were incubated overnight with fresh medium until treatments.

CT-1 (R&D Systems) was incubated at 10^{-9} mol/L for 48 h for hypertrophy assessment, 24 h for protein investigation and 3 h for mRNA analysis. To investigate the intracellular pathways involved in the CT-1 effect, the following inhibitors were added 1 h prior to addition of CT-1: PI3K inhibitor Wortmannin at 10^{-6} mol/L (Calbiochem), the MAPK inhibitor PD98059 at 10^{-6} mol/L to inhibit ERK1/2 and at 30. 10^{-6} mol/L to inhibit ERK5 (Calbiochem), the STATs inhibitor AG490 at 10^{-6} mol/L (Calbiochem), antibodies against LIFR (Santa Cruz) and gp130 (Santa Cruz) at 10^{-6} mol/L. In some experiments, cells from SHR were pre-incubated and co-incubated with the angiotensin II AT1 receptor antagonist losartan at 10^{-6} mol/L.

2.3. Image analysis

For planimetry, isolated cells were grown in glass-covered 2 cm^2 wells. After treatments, cells were fixed for 30 min in 4% formalin on ice and maintained on 70% ethanol at −20 °C until analysis. Cell area, length and width were quantified in triplicate in a minimum of 250 cardiomyocytes per experimental condition from at least 3 different rats. After digitalization at 200× magnification in an image analysis system (Soft Imaging System Analysis), cell area was calculated from the cell perimeter drawn with the mouse, cell length and cell width were drawn in triplicate as the longest and shortest axis of the cell respectively and the average was recorded. All measurements were calibrated with known standards. Myocardial determinations in cardiac tissue from 6- and 30-week-old SHR were performed in 6-μm-thick sections stained with hematoxylin for

left ventricular morphometry and with Masson trichrome for cardiomyocyte diameter. Each parameter was measured in triplicate. For cell width, at least 20 cardiomyocytes per section were measured.

2.4. Confocal microscopy

Cardiomyocytes in culture assume a cross-sectional area (CSA) that resembles a flattened ellipse. To investigate the shape changes of cardiomyocytes in 3D cells were stained with FITC (1 μg/mL) for 30 min at room temperature, washed five times in PBS and analyzed on a laser scanning confocal microscope (LSM 510, Carl Zeiss). Twenty cardiomyocytes per experimental condition were examined to obtain cell area, length and width in the *X*/*Y* plane and to analyze the CSA by means of 3D reconstruction of the cellular planes 1-μm-thick scanned in the *Z* axis. In the CSA, visualized by rotating the entire reconstructed cell around its central axis (Fig. 1A), the two diameters were computed in triplicate (*M* and *m*). Assuming an elliptical cross-section, the area of CSA was calculated as $CSA = \pi (M/2)(m/2)$. Cell volume was calculated: $V = CSA \times length$.

2.5. Assessment of sarcomeres length

For immunostaining, cells were plated in glass-covered 2 cm^2 wells. Sarcomeres were visualized by immunostaining of the Z-band α-sarcomeric actinin. Cells were fixed for 15 min at 37 °C in 3% formaldehyde. Mouse anti-α-sarcomeric actinin antibody (Sigma) was incubated for 1 h at 1:1000 in PBS and CY3-conjugated sheep anti-mouse secondary antibody (Sigma) was added for 30 min at 1:1000. After washing, cells were mounted in 4′-6-diamino-2 phenylindole (DAPI)-containing medium (Vectashield). Twenty cells per condition were captured in an epifluorescence inverted microscope and the

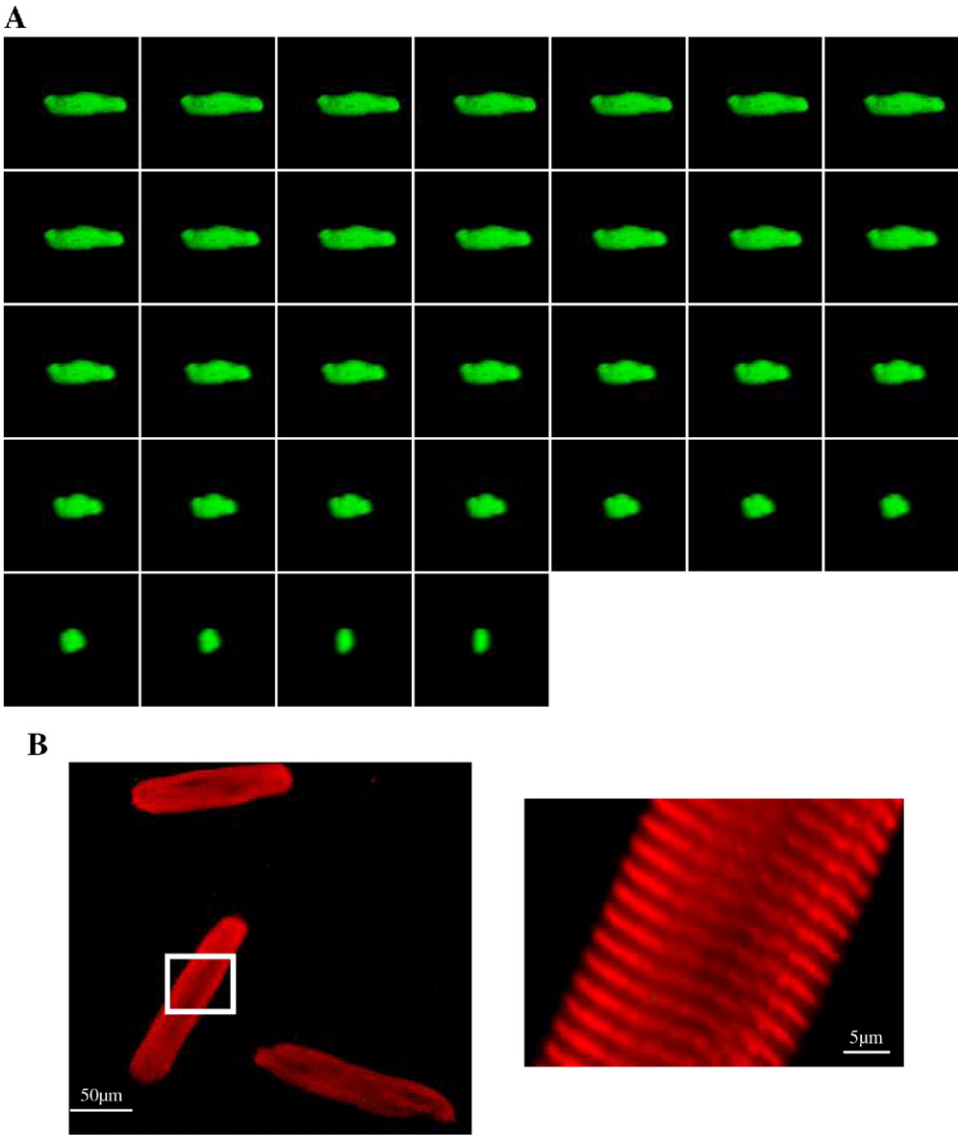

Fig. 1. (A) 3D reconstruction of an entire cardiomyocyte from 1 μm-thick plane scanned in the *Z* axis. Panels show the images obtained by rotating the reconstructed cell around the central axis. (B) α-actinin staining allowed visualizing the *Z* line located at the end of sarcomeres. Twenty cells per condition were captured and the length of 15 sarcomeres per cardiomyocyte was measured.

length of 15 sarcomeres per cardiomyocyte was measured in the Soft Imaging System Analysis.

2.6. Myofibrillar protein extraction and silver staining

Myofibrillar proteins were extracted as described by Arrel et al. [16] with minor modifications. After the specific treatments, cells were washed in PBS and harvested in 50 μL of HEPES extraction buffer consisting of (in mmol/L): HEPES 25 (pH 7.4), NaF 50, Na_3VO_4 0.25, phenylmethylsulfonyl fluoride 0.25, EDTA 0.5 and 1 tablet of protease inhibitors cocktail (Boehringer Mannheim) per 50 mL of buffer. After centrifugation, supernatants containing the cytosolic fraction were discarded and the remaining pellet was subjected to further extraction by two rounds of homogenization in 25 μL of acid extraction buffer, consisting of 1% vol/vol trifluoroacetic acid (TFA) and 1 mmol/L Tris (2-carboxyethylphosphine) hydrochloride (pH 2). Supernatants were kept at −80 °C until use. Aliquots of 5 μg of proteins were size fractionated by vertical SDS-PAGE with 15% acrylamide (200:1 acrylamide–bisacrylamide ratio, pH 9.3), and the resulting gels were silver stained according to Pharmacia Biotech's instructions. Gels were fixed in acetic acid, washed, silver stained and scanned using an image densitometer.

2.7. Western blotting

For Western blot assays, cardiomyocytes were cultured in 10 cm^2 plates. Aliquots of 20 μg of myofibrillar proteins were size fractionated on 15% (for MLC-1, MLC-2v, MLC-2-P, Troponin I and Troponin T), 12% (for p42/44 and p42/44-P) or 10% (for PI3K, PI3K-P, Akt, Akt-P, ERK5, ERK-5-P, sarcomeric α-actin and skeletal α-actin), 7.5% (for STAT-3, STAT-3-P, MHC-α, MHC-β and sarcomeric α-actinin) polyacrylamide gels by electrophoresis. The following specific antibodies were employed: MLC-1 at 1:10,000 (Abcam), MLC-2v at 1:5 (Biocytex), MLC-2v-P at 1:500 (Santa Cruz Biotechnology), Troponin I at 1:1000 (Cell Signaling), Troponin T at 1:1000 (Hytest), p42/44 1:2000 (Cell Signaling), p42/44-P (Thr202/Tyr204) at 1:4000 (Cell Signaling), PI3K at 1:1000 (Cell Signaling), PI3K-P (Tyr) at 1:1000 (Cell Signaling), Akt at 1:1000 (Cell Signaling), Akt-P (Ser473) at 1:1500 (Cell Signaling), ERK-5 at 1:1000 (Cell Signaling), ERK-5-P (Thr218/Tyr220) at 1:1000 (Cell Signaling), STAT-3 at 1:1000 (Cell Signalling), STAT-3-P (Ser727) at 1:1000 (Cell Signalling), sarcomeric α-actin at 1:10000 (Sigma), skeletal α-actin at 1:500 (Lab Vision), MHC-α at 1:200 (Covance Research), MHC-β at 1:500 (Covance Research), sarcomeric α-actinin at 1:5000 (Sigma) and CT-1 at 1:2000 (a gift from Dr. Martinez). In all cases, bound antibody was detected by peroxidase-conjugated secondary antibodies (Amersham Biosciences) and visualized using the ECL-Plus chemiluminescence detection system. After densitometric analyses, optical density values were expressed as arbitrary units (AU).

2.8. Reverse transcription and real-time PCR

Total RNA was extracted from myocytes using Trizol (Invitrogen) (1 mL/10 cm^2 dishes) and subsequently purified using QIAGEN's RNeasy Total RNA Isolation kit. Reverse transcription was performed with 250 ng of total RNA. Real-time PCR was performed with an ABI PRISM 7000 Sequence Detection System by using specific TaqMan MGB fluorescent probes (Applied BioSystems). Constitutive 18S ribosomal RNA was used as endogenous control. For the relative quantitative analysis of unknown samples, two calibration curves were prepared for both the target and the endogenous reference, representing Ct values as a function of the log amount of starting material. For each experimental condition, the mean quantity of target gene and endogenous control was obtained from the appropriate standard curve in triplicate. The SD among these triplicates was always <0.2. The mean value of target was divided by the mean value of the endogenous control to obtain a normalized mean quantity per sample or experimental condition.

Table 1
Hypertrophic effects of CT-1 in cardiomyocytes isolated from adult Wistar rats and SHR

	WISTAR			SHR		
	Baseline	CT-1	*p*	Baseline	CT-1	*p*
ANP	0.97±0.37	3.42±0.48	<0.01	2.06±0.89	8.12±0.94	<0.01
c-*fos*	7.44±2.71	19.26±2.01	<0.01	9.46±1.20	23.80±3.15	<0.01
Image analysis						
Cell area (μm²)	1796±40	2161±26	<0.01	2520±131[a]	3031±150	<0.01
Cell length (μm)	69.9±1.3	86.4±1.71	<0.01	87.0±3.5[a]	93.1±3.4	<0.05
Cell width (μm)	25.6±0.4	25.7±0.4	n.s.	32.8±1.6[a]	37.7±2.08	<0.01
Confocal microscopy						
Cell area (μm²)	1391±48	1551±71	<0.05	2197±145[a]	2976±182	<0.01
Cell length (μm)	69.7±2.6	76.2±2.5	<0.05	87.71±3.85[a]	97.14±4.8	<0.05
Cell width (μm)	22.7±1.3	22.5±1.1	n.s.	27.4±1.1[a]	34.85±1.35	<0.01
CSA (μm²)	495±34	521±48	n.s.	681±65[a]	846±49	<0.01
M (μm)	27.98±0.91	28.69±0.95	n.s.	34.08±1.79	39.56±1.50	<0.05
m (μm)	22.71±0.78	22.85±1.48	n.s.	24.98±1.20	27.11±0.90	<0.05
Volume (μm³)	35,792±3221	41,277±3143	<0.05	60,033±7696[a]	82,520±5655.77	<0.01

[a] $p<0.01$ vs. Wistar baseline. CSA: cross-sectional area. *M*: major axis of CSA. *m*: minor axis of CSA.

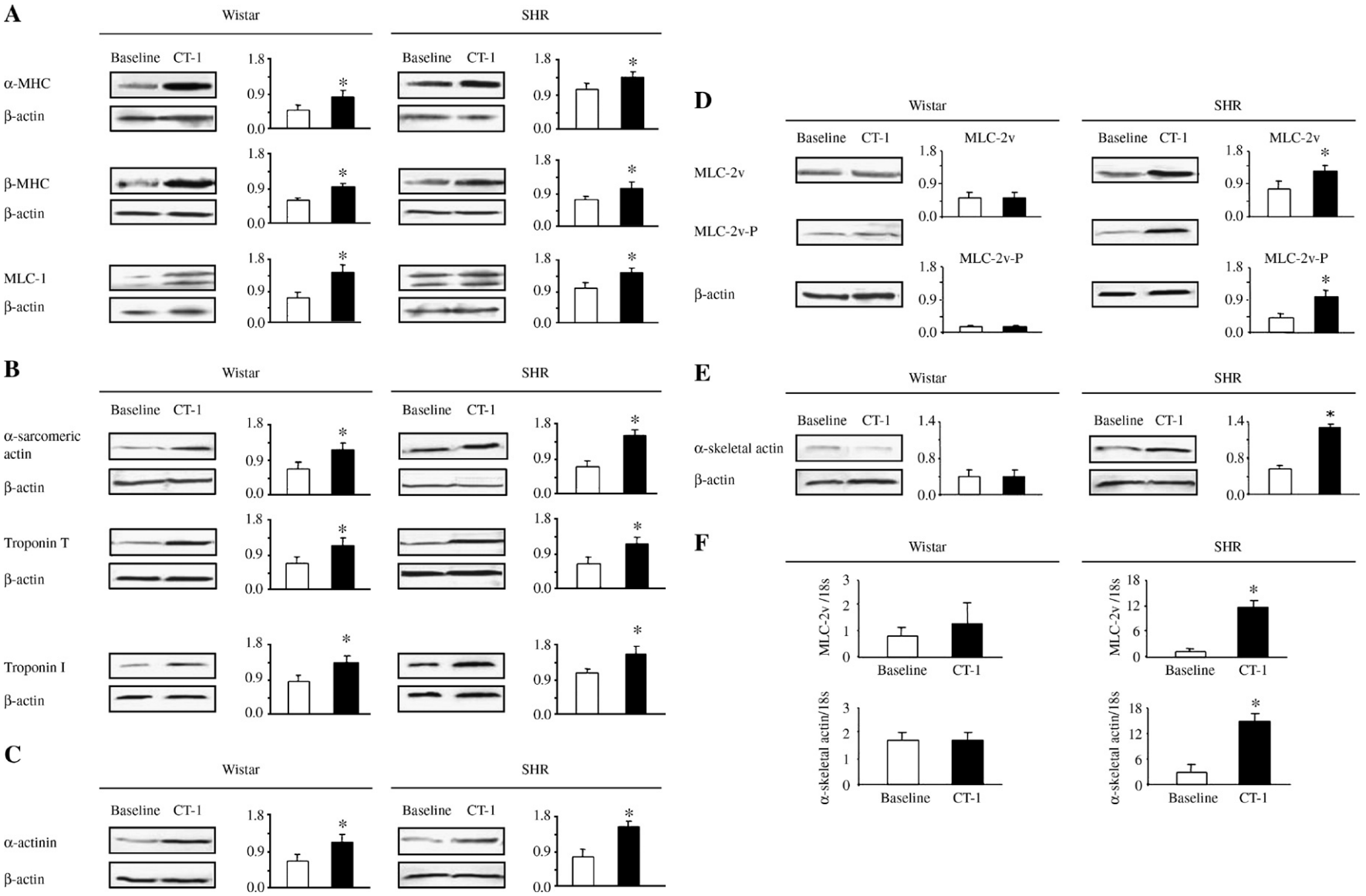

Fig. 2. CT-1 increased the expression of the shown contractile proteins from the thick filament (A), the thin filament (B) and the *Z*-band (C) of sarcomere in a similar fashion in cells from Wistar and SHR. On the contrary, CT-1 increased MLC-2v and phosphorylated MLC-2v (D) as well as skeletal α-actin (E) only in SHR cells. A representative Western blot and the histogram with bars representing the mean ± standard error of the ratio protein to β-actin obtained in three independent experiments and rats are shown for each protein. Each Western was performed at least in duplicate. (F) CT-1 increased the mRNA expression of MLC-2v and α-skeletal α-actin only in cells from SHR. The normalized mean values of the target gene are plotted. Bars represent the mean ± standard error of three independent experiments and rats. *$p<0.01$ vs. baseline.

2.9. Statistical analysis

Results are presented as mean±standard error, computed from the average measurements obtained from each group of cells or from each group of animals. Normal distribution of data was checked by means of the Shapiro Willks test. A Levene statistic test was performed to check the homogeneity of variances. Differences among more than 2 experimental conditions were tested by the ANOVA one way test followed by the Scheffé test to analyze differences between groups. The unpaired Student's *t* test or the Mann–Whitney *U* test was used to assess statistical differences between two experimental conditions and between 6- and 30-week-old SHR. *P* values lower than 0.05 were considered significant.

3. Results

3.1. CT-1 induces different morphometric patterns of hypertrophy in cardiomyocytes from Wistar rats and SHR

Hypertrophic effects of CT-1 are summarised in Table 1. Compared with cells from Wistar rats, cardiomyocytes isolated from SHR exhibited enhanced baseline expression of ANP and c-*fos* mRNA expression ($p<0.05$) and greater cell area ($p<0.01$), cell width ($p<0.01$) and cell length ($p<0.01$) assayed by means of both conventional image analysis and confocal microcopy. Baseline CSA and cell volume determined by confocal microscopy were also higher in cells from SHR ($p<0.01$). Incubation with CT-1 resulted in the increase of ANP and c-*fos*, cell area and length in the two cell types. However, cell width, assayed by image analysis or confocal microscopy, and cell depth and CSA determined by confocal microscopy were augmented by CT-1 only in SHR cells (Table 1). Similar results were found in cardiomyocytes isolated from Wistar and SHR with different ages (from 6 to 25 weeks old), suggesting that the specific morphometry observed in SHR cardiomyocytes did not depend on the baseline cardiomyocyte size (data not shown).

Visualization of sarcomeric Z-bands by α-sarcomeric actinin staining (Fig. 1B) allowed determining sarcomere length to verify that CT-1 did not modify this parameter (baseline: 2.49±0.08 μm, CT-1: 2.48±0.02 μm). These experiments were performed in cells from Wistar rats, given that they exhibited the highest elongation response.

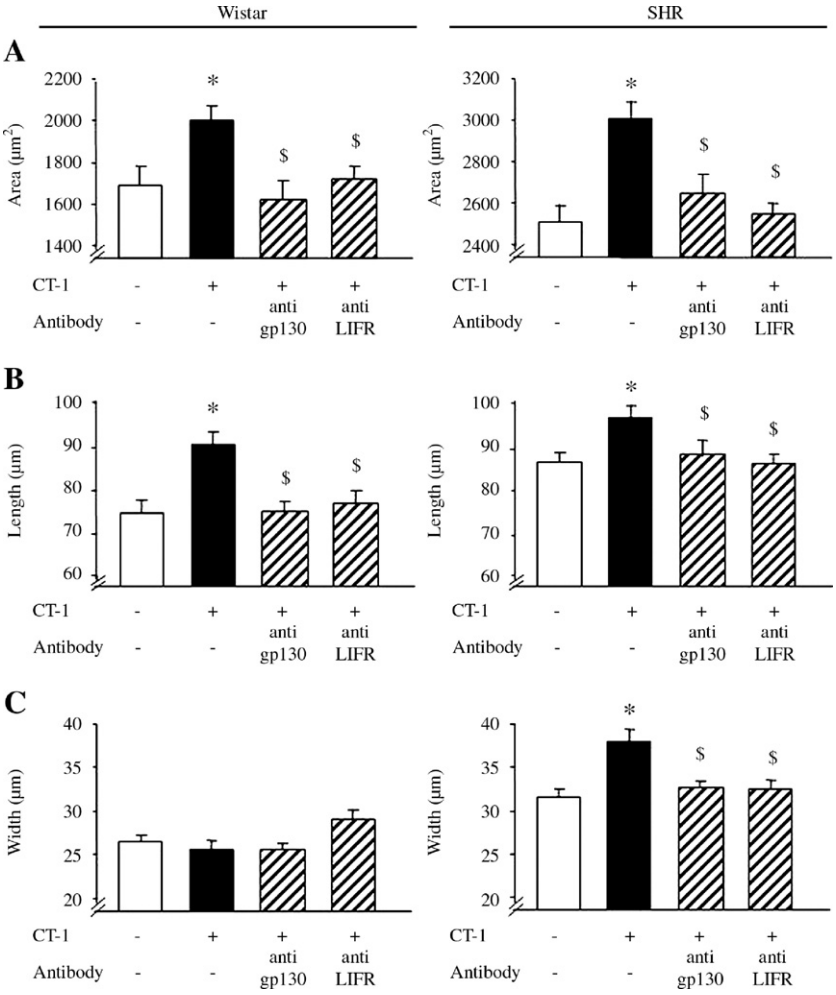

Fig. 3. Cell area (A), length (B) and width (C) were determined by planimetry after pre-incubation for 1 h with antibodies specific for gp130 or LIFR and incubation with CT-1 for 48 h. Values represent the mean±standard error of a minimum of 120 cardiomyocytes per experimental condition. Three independent experiments performed in three rats yielded identical results. *$p<0.01$ vs. baseline; \$$p<0.01$ vs. CT-1 without antibody.

3.2. CT-1 induces distinct molecular patterns of contractile protein expression in cardiomyocytes from Wistar rats and SHR

Silver-stained gels of high-abundance proteins illustrated that CT-1 promoted a different pattern of contractile protein expression in Wistar rats and SHR cardiomyocytes (data not shown). Thus, CT-1-induced changes in the expression of the main contractile proteins were assayed by Western blotting in cardiomyocytes from the two strains. Panels A–C in Fig. 2 show that CT-1 enhanced ($p<0.05$) in a similar manner the expression of α- and β-MHC, MLC-1, sarcomeric α-actin, Troponins I and T and sarcomeric α-actinin in cardiomyocytes isolated from Wistar rats and SHR. In contrast, CT-1 augmented ($p<0.01$) the amount of MLC-2v, phosphorylated MLC-2v and skeletal α-actin only in cardiomyocytes from SHR, while no changes were observed in cells from Wistar rats (Fig. 2D, E). The analysis of mRNA expression by real-time RT-PCR confirmed that the specific changes in these proteins were produced at transcriptional level since both MLC-2v and skeletal α-actin mRNAs were significantly augmented by CT-1 in SHR cells ($p<0.01$) (Fig. 2F).

3.3. Signaling pathways mediating CT-1 hypertrophic responses in cardiomyocytes from Wistar rats and SHR

We further explored the origin of the distinct CT-1 effects observed in SHR cells by analyzing the signaling pathways triggered by the cytokine. To investigate the involvement of gp130/LIFR heterodimer, cardiomyocytes from the two strains were incubated with specific antibodies against the two subunits prior to the addition of the cytokine. As illustrated in Fig. 3, the presence of any of the two antibodies abolished ($p<0.01$) the increment in cell area and length induced by CT-1 alone in cells from the two strains of rats, and it also abrogated the increment in cell width observed in cardiomyocytes from SHR. The quantitative analysis of gp130 and LIFR mRNA and protein in cardiomyocytes from Wistar rats and SHR demonstrated a similar expression of these molecules in the cells from the two strains of rats (data not shown). Phosphorylation assessment of the main known CT-1 intermediates demonstrated an enhanced baseline activation of STAT3 and ERK5 in cardiomyocytes from SHR compared to cells from Wistar rats ($p<0.01$) (Fig. 4). Incubation with CT-1 promoted the phosphorylation of the five signaling substrates analyzed (PI3K, Akt, p42/44, STAT3 and ERK5) in the two groups of cardiomyocytes (Fig. 4), indicating that CT-1 activates the same intracellular pathways in cells from the two strains of rats. The higher ($p<0.01$) increase in STAT3 and ERK5 phosphorylation observed in SHR cardiomyocytes might be due to the enhanced baseline phosphorylation observed in these substrates. To study the involvement of these signaling pathways in CT-1-induced hypertrophy, specific chemical inhibitors were added to the culture medium prior to the addition of the cytokine. As shown in Fig. 5, both MEK5 inhibition with PD98059 30 μmol/L and STAT3 inhibition with AG490 abolished ($p<0.01$) the increment in cell area and length induced by CT-1 in Wistar rats and

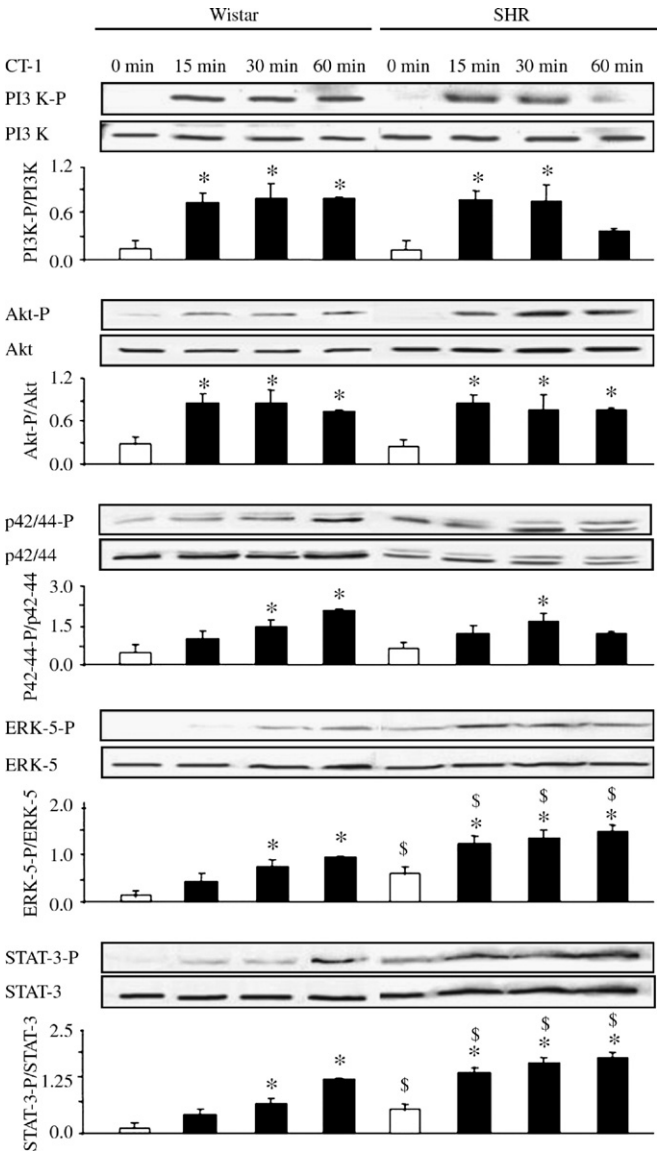

Fig. 4. Cardiomyocytes were incubated with CT-1 for the indicated times. Proteins from Wistar rats and SHR cardiomyocytes were analyzed in the same membrane. Images are representative of three independent experiments, and histograms bars represent the mean±standard error of the three independent experiments performed with three rats. *$p<0.01$ vs. CT-1 baseline (0 min); \$$p<0.05$ vs. Wistar activation.

SHR cells. In contrast, only AG490 blunted ($p<0.05$) the increase in transverse diameter observed in SHR cells. Neither PI3K inhibition with Wortmannin nor p42/44 inhibition with PD98059 1 μmol/L affected the hypertrophic effects of CT-1. None of the chemical inhibitors employed modified cardiomyocyte dimensions when incubated alone (data not shown). As shown in Fig. 6A, the increase in MLC-2v and skeletal α-actin induced by CT-1 in SHR cardiomyocytes was abrogated by AG490, indicating that STAT3 mediated this specific effect in these cells. The induction of angiotensinogen mRNA expression by CT-1 via STAT3 has been previously reported in neonatal cardiomyocytes [17], but this effect had not been tested in adult cells. Given that the distinct response observed in SHR cells appeared to be mediated by STAT3 pathway, we compared the

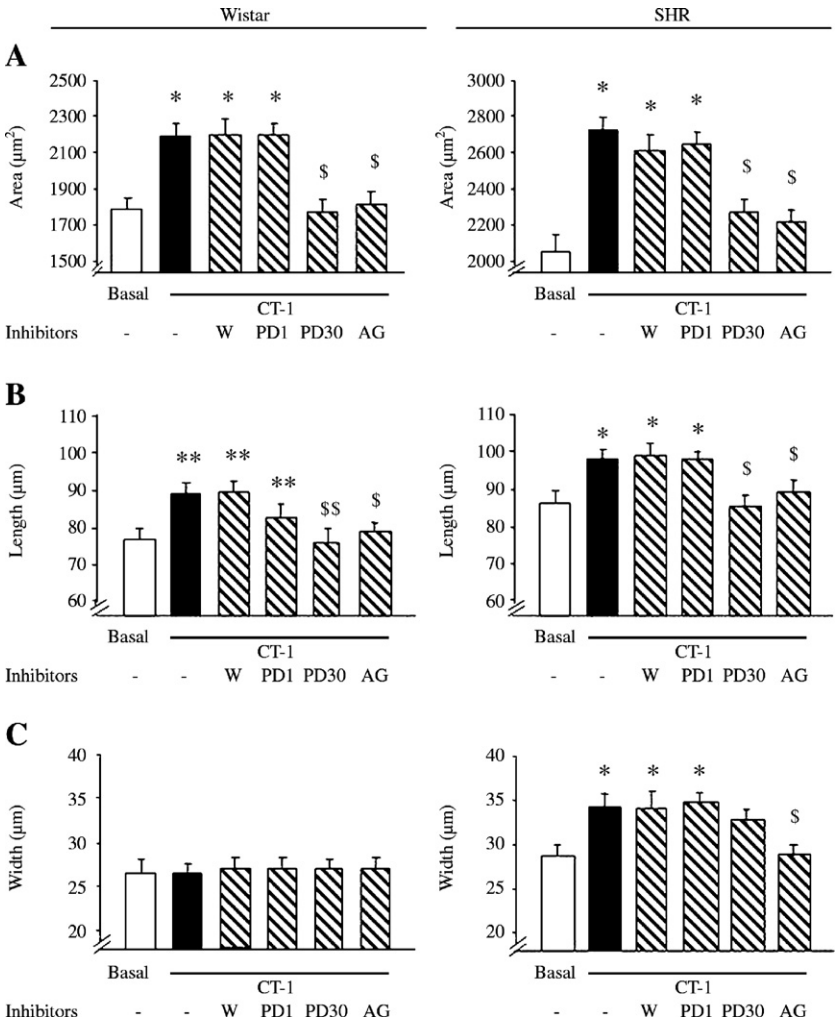

Fig. 5. Cells were pre-incubated with the indicated chemical inhibitors for 1 h and then with CT-1 for 48 h. Cell area (A), length (B) and width (C) were determined by planimetry. Values represent the mean ± standard error of a minimum of 120 cardiomyocytes per experimental condition. Three independent experiments performed in three rats yielded identical results. $^{**}p<0.01$ vs. baseline; $^{*}p<0.05$ vs. baseline; $\$\$p<0.01$ vs. CT-1; $\$p<0.05$ vs. CT-1. W, Wortmannin; PD1, PD98059 at 10^{-6} mol/L to inhibit p42/44; PD30, PD98059 at 30×10^{-6} mol/L to inhibit ERK-5; AG, AG490.

induction of angiotensinogen expression by CT-1 in cells from the two strains of rats. Fig. 6B illustrates that cardiomyocytes from SHR exhibited higher ($p<0.01$) baseline expression of angiotensinogen compared to cardiomyocytes from Wistar rats. CT-1 induced a 1.7-fold increase ($p<0.01$) in cells from Wistar rats and a 3.2-fold increase ($p<0.01$) in cells from SHR. Hence, angiotensinogen expression after CT-1 incubation was 3.8-fold increased in SHR cardiomyocytes compared to cells from Wistar rats. Finally, co-incubation of SHR cardiomyocytes with CT-1 and losartan inhibited the increase in angiotensinogen expression, cell width and MLC-2v and skeletal-α-actin expression induced by CT-1 alone in these cells (Fig. 7).

3.4. Myocardial expression of CT-1 is associated with cardiomyocyte growth and left ventricular hypertrophy in SHR

To study whether the differential hypertrophic effect observed in SHR cardiomyocytes had a relevance *in vivo*, myocardial expression of CT-1, cardiomyocyte width and left ventricle geometry were assayed in 6- and 30-week-old SHR. Compared with young animals, 30-week-old SHR exhibited enhanced blood pressure (233±4 vs. 180±4 mm Hg, $p<0.01$) and cardiac weight (1.9±0.01 vs. 0.46±0.02 g, $p<0.01$). Myocardial expression of CT-1 mRNA and protein was augmented ($p<0.01$) in 30-week-old SHR compared to 6-week-old SHR (Fig. 8A). Transverse diameter of cardiomyocytes was significantly increased in 30-week-old SHR compared with 6-week-old SHR (46.1±1.5 μm vs. 27.0±0.9 μm, $p<0.01$). The ratio left ventricular wall thickness to left ventricular chamber diameter was 1.7-fold higher ($p<0.01$) in 30-week-old SHR compared with 6-week-old SHR (Fig. 8B). Similarly, the ratio left ventricular cross-sectional area to left ventricular chamber area was 2.4-fold increased ($p<0.01$) in 30-week-old SHR compared to 6-week-old SHR. These data indicate that SHR developed concentric LVH.

4. Discussion

The main findings of the current study are the following: first, CT-1 promotes longitudinal elongation of normal adult

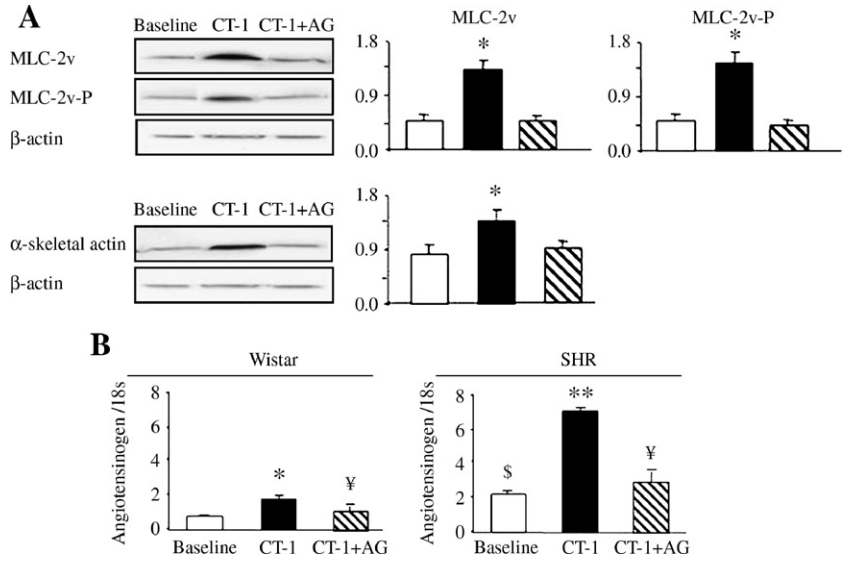

Fig. 6. (A) SHR cardiomyocytes were pre-incubated for 1 h with the STAT3 blocker AG490 and then with CT-1 for 24 h. A representative Western blot and the histogram with bars representing the mean±standard error of three independent experiments are shown for each protein. *$p<0.01$ vs. baseline and CT-1+AG. AG, AG490 (B) Angiotensinogen mRNA was assayed in cardiomyocytes from Wistar rats and SHR before and after 3 h incubation with CT-1. Bars represent mean±standard error of triplicates in three independent experiments. \$$p<0.01$ vs. baseline; *$p<0.01$ vs. CT-1.

cardiomyocytes via gp130/LIFR and downstream mediation of STAT3 and MEK5. Second, in cardiomyocytes from adult SHR, CT-1 specifically augments cell length and width, the expression of MLC-2v and skeletal α-actin and the phosphorylation degree of MLC-2v. All these actions are mediated by STAT3 signaling cascade. Third, the distinct effects observed in SHR cardiomyocytes are associated with the higher CT-1-induced angiotensinogen expression detected in these cells, and they are inhibited by the AT_1 receptor antagonist losartan. Finally, an exaggerated expression of myocardial CT-1 is temporally associated with cardiomyocyte widening during the development of concentric hypertrophy in SHR.

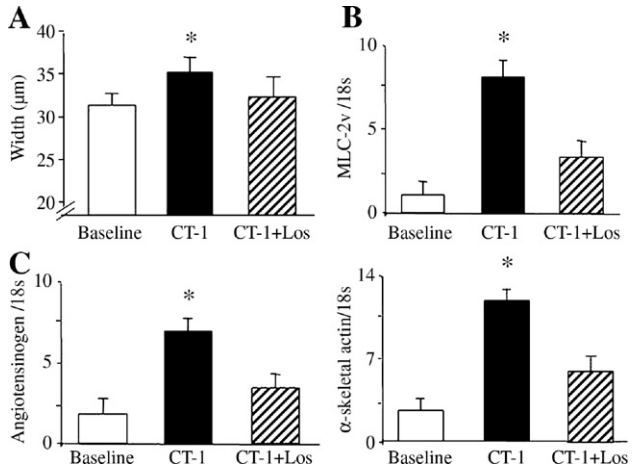

Fig. 7. SHR cardiomyocytes were pre-incubated for 1 h with the AT1 blocker losartan and then with CT-1 for 24 h (A) or 3 h (B) and (C). Cell width was assayed by planimetry, and mRNA expression of the indicated genes was assayed by real-time RT-PCR. The normalized mean values of the target genes are plotted in (B) and (C). Bars represent the mean±standard error of three independent experiments performed in three rats. *$p<0.01$ vs. baseline and CT-1+Los.

Current data in cells from Wistar rats are the first evidence showing that CT-1 induces a longitudinal pattern of enlargement together with the absence of changes in the expression of skeletal α-actin and MLC-2v in adult cardiomyocytes. The observation that CT-1 does not modify the length of sarcomeres indicates that the increase in cell length results from the addition of new myofibrils in series. These findings are in accordance with previous studies performed in neonatal cells by Wollert et al. [12]. We also show that the blockade of STAT3 or MEK5 blunts the hypertrophic effect of CT-1. The involvement of MEK5 in CT-1-induced longitudinal elongation has been recently reported in neonatal cardiomyocytes [18], and it is further supported by the molecular observation that overexpression of activated MEK5 induces serial insertion of sarcomeres in neonatal cardiomyocytes *in vitro* and eccentric cardiac hypertrophy *in vivo* [19]. With regard to the STAT3 pathway, although it is reportedly involved in neonatal cardiomyocyte hypertrophy induced by CT-1 [11] and other IL-6-related cytokines [4], its role has been recently questioned by other authors in the same cell type [18]. Interestingly, STAT3 upregulates MEK5 in other cell types [20]. Thus, the possibility that STAT3 mediates the longitudinal elongation through the downstream activation of MEK5, which determines the serial assembly of sarcomeres, requires further investigations.

The main finding in the present study is the distinct effect of CT-1 observed in SHR cardiomyocytes. The most important determinant of LVH in SHR is the transverse growth of cardiomyocytes, which has been previously reported both in cardiac tissue and in isolated cells [21,22]. Similarly, other groups have demonstrated an increase mRNA expression of the contractile protein MLC-2v [23,24] and the embryonic gene skeletal α-actin [25] in this experimental model. Several cardiomyocyte growth factors, including endothelin, angiotensin II and α-adrenergic stimulation, upregulate the expression of

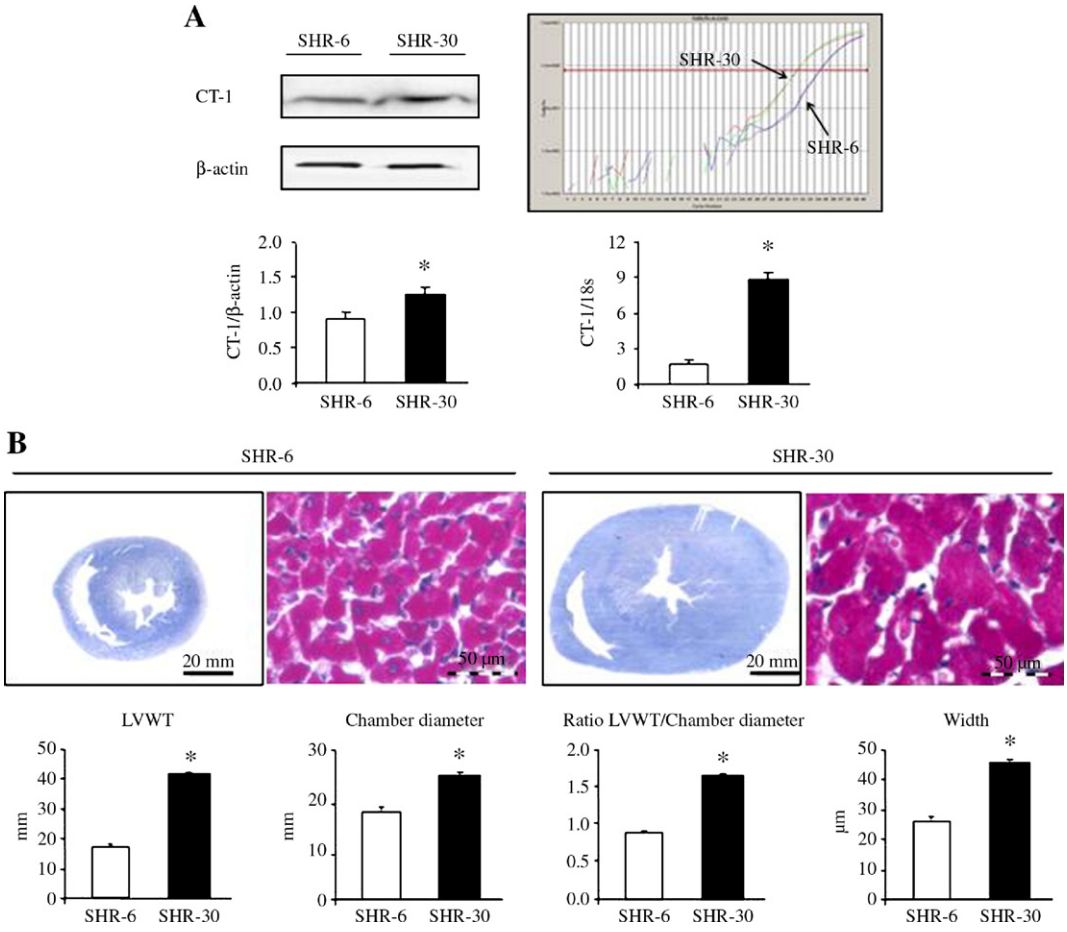

Fig. 8. (A) The expression of CT-1 was determined in myocardium from 6-week-old SHR (SHR-6, $N=10$) and 30-week-old SHR (SHR-30, $N=10$). A representative Western blot and PCR are shown in the upper panels, and the histogram bars represent mean ± standard error in each group. (B) Left ventricle morphometry and cardiomyocyte transverse diameter were assayed in 6 μm tissue sections stained with hematoxylin and Masson trichrome respectively. All parameters were determined in triplicate. For cardiomyocyte width, at least 20 cells per section were measured. Representative tissue sections employed for left ventricular morphometry and cardiomyocyte diameter analysis are shown in the upper panels. Histogram bars represent the mean ± standard error obtained in the two groups of animals ($N=10$). LVWT: left ventricle wall thickness; *$p<0.01$ vs. 6-week-old SHR.

MLC-2v [26–29] and skeletal α-actin [30–32]. Thus, current data suggest that CT-1 is a new specific cellular inducer of SHR cardiomyocyte growth and, hence, a new potential mediator of LVH in hypertension. Of special interest is the observation that CT-1 increases MLC-2v phosphorylation. Phosphorylated MLC-2v activates the contraction in smooth muscle and modulates force production in striated muscle. Several biochemical studies have demonstrated that this chemical modification, which produces a change in charge affecting the amino-terminus of the protein, potentiates productive interactions of the myosin head with the actin filament and leads to increased calcium sensitivity [33]. In addition, the observation that transgenic mice expressing non-phosphorylable MLC-2v in the ventricle develop cardiac dilatation suggests a role for this modification of MLC-2v in normal cardiac development and maintenance [34]. Interestingly, phosphorylation of MLC-2v by MLC kinase has been reported to mediate sarcomere organization in neonatal cardiomyocytes in response to hypertrophic agonists [35], however, its role in the insertion of sarcomeres that account in the adult cell has not been investigated. The precise involvement of phosphorylated MLC-2v in the transverse growth of adult cardiomyocytes and the pathophysiological meaning of this molecule in pressure overload LVH should be further studied.

The question arises as to the molecular mechanisms determining the distinct CT-1 effects observed in SHR cells. Current data comparing the signaling cascade triggered by CT-1 show that the cytokine activates by phosphorylation the same intracellular pathways in cardiomyocytes from Wistar rats and SHR. Moreover, in both cases, hypertrophy is induced via gp130/LIFR heterodimer and involves the same downstream cascades, namely STAT3 and MEK5 mediating the increase in cell area and length size. Finally, the expression of gp130 and LIFR is similar in cells from the two strains of rats. Taken together, these results indicate that the specific response of cardiomyocytes from SHR to CT-1 may be downstream the mediators here analyzed. The observation that all the specific effects found in SHR are abolished by the STAT3 inhibitor AG490 suggests a role of this signaling cascade in the distinct response of these cells. STATs are transcription factors that mediate cytokine and growth factor-induced gene transcription. Ligand binding to

gp130 promotes JAKs phosphorylation that in turn phosphorylates in tyrosine the STAT3 located in the cytoplasm. Activated STAT3 translocates to the nucleus, binds to specific DNA response sequences and triggers the expression of target genes. A growing line of evidence has implicated the gp130 activation of JAK/STAT cascade in pressure overload cardiac hypertrophy [36,37]. Specifically, CT-1 increases angiotensinogen promoter activity and mRNA expression in rat cardiomyocytes through STAT3 phosphorylation and subsequent binding to the specific St-domain [17]. Interestingly, the St-binding activity of STAT3 is dramatically increased in hypertrophied hearts from adult SHR, probably because of the local activation of renin–angiotensin system that accounts in this model since angiotensin II injection *in vivo* mimics the enhanced St-binding activity of STAT3 observed in the myocardium of SHR [38]. Current results showing enhanced STAT3 phosphorylation and angiotensinogen expression in SHR cardiomyocytes, both at baseline conditions and after CT-1 incubation, are in accordance with the over-activation of this signaling pathway and its final effect in this experimental model. Moreover, the observation that the AT1 antagonist losartan inhibits all the specific effects that CT-1 exerts in SHR cardiomyocytes strongly reinforces the possibility that a cross-talk with the renin–angiotensin system mediates the distinct hypertrophic effects of CT-1 in cardiomyocytes with hypertensive phenotype, via an exaggerated induction of angiotensinogen expression which may lead to the participation of angiotensin II in cell growth. This hypothesis is further supported by previous evidences showing that the octepeptide increases cardiomyocyte width, enhances MLC-2v and skeletal α-actin expression in isolated cardiomyocytes [27,30] and promotes MLC-2v phosphorylation both *in vitro* and *in vivo* [35].

At the structural level, the increase in cardiomyocyte length results from the addition of sarcomeres in series and is characteristic of volume overload cardiac hypertrophy [39], whereas the insertion of new sarcomeric units in parallel produces the transverse enlargement of cardiomyocytes present in pressure overload hypertrophy [40]. Moreover, normal myocardial levels of skeletal α-actin have been reported in volume overload states, whereas pressure overload seems to be associated with enhanced levels of this fetal protein [41,42]. Present findings in Wistar adult cells reinforce conceit that the cell growth induced by CT-1 in normal cardiomyocytes resembles volume overload hypertrophy. However, recent experimental [5,14] and clinical [5,6] evidence indicates that CT-1 may be involved in hypertensive LVH. Our *ex vivo* data show for the first time a temporal association between the increase in myocardial CT-1 expression (mRNA and protein) and cardiomyocyte widening during the development of concentric LVH in SHR, reinforcing a role for this cytokine in hypertrophy that accounts in genetic hypertension. In addition, present *in vitro* data provide a molecular explanation to understand how the specific hypertensive phenotype of SHR cardiomyocytes determines their distinct response to growth factors such as CT-1.

In summary, we demonstrate for the first time that CT-1 exerts specific hypertrophic effects in cardiomyocytes from SHR compared to cardiomyocytes from adult Wistar rats, namely: the increase in cell width, the increase in MLC-2v and skeletal α-actin expression and the enhanced phosphorylation of MLC-2v. Our data suggest that the molecular origin of this differential effect is downstream STAT3 pathway activation and involve the over-induction of rennin–angiotensin system. We also show an association of enhanced myocardial CT-1 expression with cardiomyocyte transverse growth and concentric LVH in SHR. This observation strengthens a potential role for this cytokine in the pressure overload hypertrophy that develops this genetic model of hypertension and, likely, in essential hypertension. We conclude that CT-1-induced hypertrophy critically depends on cardiomyocyte hypertensive phenotype. Future studies modifying myocardial CT-1 expression should confirm the pathogenetic involvement of the cytokine in hypertensive heart disease.

Acknowledgments

We thank Dr. E. Martínez (Division of Gene Therapy and Hepatology, CIMA, Pamplona, Spain) for providing us the rat CT-1 polyclonal antibody. Manuscript comments from Dr. G. Zalba and Dr. N. Varo (Division of Cardiovascular Sciences, CIMA, Pamplona, Spain) are greatly appreciated. We especially thank the technical assistance from S. Martínez in the confocal microscope. This study was supported by the UTE project of CIMA, by a grant from the Ministry of Health (FIS 02/1484) and by a grant from the Ministry of Science and Technology, PROFIT program (FIT 090000-20-30108).

References

[1] Fedak PW, Verma S, Weisel RD, Li RK. Cardiac remodeling and failure: from molecules to man (Part I). Cardiovasc Pathol 2005;14:1–11.
[2] Hunter JJ, Chien KR. Signaling pathways for cardiac hypertrophy and failure. N Engl J Med 1999;341:1276–83.
[3] Lips DJ, deWindt LJ, van Kraaij DJ, Doevendans PA. Molecular determinants of myocardial hypertrophy and failure: alternative pathways for beneficial and maladaptive hypertrophy. Eur Heart J 2003;24:883–96.
[4] Kunisada K, Tone E, Fujio Y, Matsui H, Yamauchi-Takihara K, Kishimoto T. Activation of gp130 transduces hypertrophic signals via STAT3 in cardiac myocytes. Circulation 1998;98:346–52.
[5] Pemberton CJ, Raudsepp SD, Yandle TG, Cameron VA, Richards AM. Plasma cardiotrophin-1 is elevated in human hypertension and stimulated by ventricular stretch. Cardiovasc Res 2005;68(1):109–17.
[6] Lopez B, Gonzalez A, Lasarte JJ, Sarobe P, Borras F, Diaz A, et al. Is plasma cardiotrophin-1 a marker of hypertensive heart disease? J Hypertens 2005;23:625–32.
[7] Pennica D, Shaw KJ, Swanson TA, Moore MW, Shelton DL, Zioncheck KA, et al. Cardiotrophin-1. Biological activities and binding to the leukemia inhibitory factor receptor/gp130 signaling complex. J Biol Chem 1995;270:10915–22.
[8] Liao Z, Brar BK, Cai Q, Stephanou A, O'Leary RM, Pennica D, et al. Cardiotrophin-1 (CT-1) can protect the adult heart from injury when added both prior to ischaemia and at reperfusion. Cardiovasc Res 2002;53:902–10.
[9] Lopez N, Diez J, Fortuno MA. Characterization of the protective effects of cardiotrophin-1 against non-ischemic death stimuli in adult cardiomyocytes. Cytokine 2005;30:282–92.
[10] Pennica D, King KL, Shaw KJ, Luis E, Rullamas J, Luoh SM, et al. Expression cloning of cardiotrophin 1, a cytokine that induces cardiac myocyte hypertrophy. Proc Natl Acad Sci U S A 1995;92:1142–6.
[11] Railson JE, Liao Z, Brar BK, Buddle JC, Pennica D, Stephanou A, et al.

Cardiotrophin-1 and urocortin cause protection by the same pathway and hypertrophy via distinct pathways in cardiac myocytes. Cytokine 2002;17:243–53.
[12] Wollert KC, Taga T, Saito M, Narazaki M, Kishimoto T, Glembotski CC, et al. Cardiotrophin-1 activates a distinct form of cardiac muscle cell hypertrophy. Assembly of sarcomeric units in series via gp130/leukemia inhibitory factor receptor-dependent pathways. J Biol Chem 1996; 271:9535–45.
[13] Jin H, Yang R, Keller GA, Ryan A, Ko A, Finkle D, et al. In vivo effects of cardiotrophin-1. Cytokine 1996;8:920–6.
[14] Ishikawa M, Saito Y, Miyamoto Y, Harada M, Kuwahara K, Ogawa E, et al. A heart-specific increase in cardiotrophin-1 gene expression precedes the establishment of ventricular hypertrophy in genetically hypertensive rats. J Hypertens 1999;17:807–16.
[15] Gonzalez A, López B, Martín-Raymondi D, Lozano E, Varo N, Barba J, et al. Usefulness of plasma cardiotrophin-1 in assessment of left ventricular hypertrophy regression in hypertensive patients. J Hypertens 2005;23:2293–300.
[16] Arrell DK, Neverova I, Fraser H, Marban E, Van Eyk JE. Proteomic analysis of pharmacologically preconditioned cardiomyocytes reveals novel phosphorylation of myosin light chain 1. Circ Res 2001;89:480–7.
[17] Fukuzawa J, Booz GW, Hunt RA, Shimizu N, Karoor V, Baker KM, et al. Cardiotrophin-1 increases angiotensinogen mRNA in rat cardiac myocytes through STAT3: an autocrine loop for hypertrophy. Hypertension 2000;35:1191–6.
[18] Takahashi N, Saito Y, Kuwahara K, Harada M, Tanimoto K, Nakagawa Y, et al. Hypertrophic responses to cardiotrophin-1 are not mediated by STAT3, but via a MEK5-ERK5 pathway in cultured cardiomyocytes. J Mol Cell Cardiol 2005;38:185–92.
[19] Nicol RL, Frey N, Pearson G, Cobb M, Richardson J, Olson EN. Activated MEK5 induces serial assembly of sarcomeres and eccentric cardiac hypertrophy. EMBO J 2001;20:2757–67.
[20] Song H, Jin X, Lin J. Stat3 upregulates MEK5 expression in human breast cancer cells. Oncogene 2004;23:8301–9.
[21] Bell D, Kelso EJ, Argent CC, Lee GR, Allen AR, McDermott BJ. Temporal characteristics of cardiomyocyte hypertrophy in the spontaneously hypertensive rat. Cardiovasc Pathol 2004;13:71–8.
[22] Onodera T, Tamura T, Said S, McCune SA, Gerdes AM. Maladaptive remodeling of cardiac myocyte shape begins long before failure in hypertension. Hypertension 1998;32:753–7.
[23] Kumar CC, Cribbs L, Delaney P, Chien KR, Siddiqui MA. Heart myosin light chain 2 gene. Nucleotide sequence of full length cDNA and expression in normal and hypertensive rat. J Biol Chem 1986; 261:2866–72.
[24] Kumar C, Saidapet C, Delaney P, Mendola C, Siddiqui MA. Expression of ventricular-type myosin light chain messenger RNA in spontaneously hypertensive rat atria. Circ Res 1988;62:1093–7.
[25] Dalton GR, Jones JV, Levi AJ, Levy A. Changes in contractile protein gene expression with ageing and with captopril-induced regression of hypertrophy in the spontaneously hypertensive rats. J Hypertens 2000; 18:1297–306.
[26] King KL, Winer J, Phillips DM, Quach J, Williams PM, Mather JP. Phenylephrine, endothelin, prostaglandin F2alpha′ and leukemia inhibitory factor induce different cardiac hypertrophy phenotypes in vitro. Endocrine 1998;9:45–55.
[27] Mathew S, Mascareno E, Siddiqui MA. A ternary complex of transcription factors, Nished and NFATc4, and co-activator p300 bound to an intronic sequence, intronic regulatory element, is pivotal for the up-regulation of myosin light chain-2v gene in cardiac hypertrophy. J Biol Chem 2004; 279:41018–27.
[28] Shubeita HE, Martinson EA, Van Bilsen M, Chien KR, Brown JH. Transcriptional activation of the cardiac myosin light chain 2 and atrial natriuretic factor genes by protein kinase C in neonatal rat ventricular myocytes. Proc Natl Acad Sci U S A 1992;89:1305–9.
[29] Lee HR, Henderson SA, Reynolds R, Dunnmon P, Yuan D, Chien KR. Alpha 1-adrenergic stimulation of cardiac gene transcription in neonatal rat myocardial cells. Effects on myosin light chain-2 gene expression. J Biol Chem 1988;263:7352–8.
[30] Clement S, Chaponnier C, Gabbiani G, Pellieux C, Pedrazzini T. Angiotensin II stimulates-skeletal actin expression in cardiomyocytes in vitro and in vivo in the absence of hypertension. Differentiation 2001; 69:66–74.
[31] Munzel F, Muhlhauser U, Zimmermann WH, Didie M, Schneiderbanger K, Schubert P, et al. Endothelin-1 and isoprenaline co-stimulation causes contractile failure which is partially reversed by MEK inhibition. Cardiovasc Res 2005;68:464–74.
[32] Jeong MY, Kinugawa K, Vinson C, Long CS. AFos dissociates cardiac myocyte hypertrophy and expression of the pathological gene program. Circulation 2005;111:1645–51.
[33] Patel JR, Diffee GM, Moss RL. Myosin regulatory light chain modulates the Ca2+ dependence of the kinetics of tension development in skeletal muscle fibers. Biophys J 1996;70:2333–40.
[34] Sanbe A, Fewell JG, Gulick J, Osinska H, Lorenz J, Hall DG, et al. Abnormal cardiac structure and function in mice expressing nonphosphorylatable cardiac regulatory myosin light chain 2. J Biol Chem 1999;274:21085–94.
[35] Aoki H, Sadoshima J, Izumo S. Myosin light chain kinase mediates sarcomere organization during cardiac hypertrophy in vitro. Nat Med 2000;6:183–8.
[36] Pan J, Fukuda K, Kodama H, Sano M, Takahashi T, Makino S, et al. Involvement of gp130-mediated signaling in pressure overload-induced activation of the JAK/STAT pathway in rodent heart. Heart Vessels 1998;13:199–208.
[37] Kuwahara K, Saito Y, Harada M, Ishikawa M, Ogawa E, Miyamoto Y, et al. Involvement of cardiotrophin-1 in cardiac myocyte–nonmyocyte interactions during hypertrophy of rat cardiac myocytes in vitro. Circulation 1999;100:1116–24.
[38] Mascareno E, Dhar M, Siddiqui MAQ. Signal transduction and activator of transcription (STAT) protein-dependent activation of angiotensinogen promoter: a cellular signal for hypertrophy in cardiac muscle. PNAS 1998;95:5590–4.
[39] Anversa P, Levicky V, Beghi C, McDonald SL, Kikkawa Y. Morphometry of exercise-induced right ventricular hypertrophy in the rat. Circ Res 1983;52:57–64.
[40] Anversa P, Olivetti G, Melissari M, Loud AV. Stereological measurement of cellular and subcellular hypertrophy and hyperplasia in the papillary muscle of adult rat. J Mol Cell Cardiol 1980;12:781–95.
[41] Calderone A, Takahashi N, Izzo Jr NJ, Thaik CM, Colucci WS. Pressure- and volume-induced left ventricular hypertrophies are associated with distinct myocyte phenotypes and differential induction of peptide growth factor mRNAs. Circulation 1995;92:2385–90.
[42] Yoshihara F, Nishikimi T, Horio T, Yutani C, Nagaya N, Matsuo H, et al. Ventricular adrenomedullin concentration is a sensitive biochemical marker for volume and pressure overload in rats. Am J Physiol Heart Circ Physiol 2000;278:H633–42.